the plant journal

SEB SOCIETY FOR EXPERIMENTAL BIOLOGY

The Plant Journal (2008) **55**, 832–843 doi: 10.1111/j.1365-313X.2008.03552.x

SOC1 translocated to the nucleus by interaction with AGL24 directly regulates *LEAFY*

Jungeun Lee[1], Mijin Oh[1], Hanna Park[1] and Ilha Lee[1,2,3,*]

[1]*National Research Laboratory of Plant Developmental Genetics, Department of Biological Sciences, Seoul National University, Seoul, 151-742, Korea,*

[2]*Global Research Laboratory for Flowering in Seoul National University, Seoul, 151-742, Korea, and*

[3]*Plant Metabolism Research Center, Kyung Hee University, Suwon 449-701, Korea*

Received 24 February 2008; revised 21 April 2008; accepted 1 May 2008; published online 13 June 2008.

*For correspondence (fax +82-2-872-6950; e-mail ilhalee@snu.ac.kr).

Summary

***SUPPRESSOR OF OVEREXPRESSION OF CONSTANS1* (*SOC1*) is one of the flowering pathway integrators and regulates the expression of *LEAFY* (*LFY*), which links floral induction and floral development. However, the mechanism by which SOC1, a MADS box protein, regulates *LFY* has proved elusive. Here, we show that SOC1 directly binds to the distal and proximal region of the *LFY* promoter where critical *cis*-elements are located. Intragenic suppressor mutant analysis shows that a missense mutation in the MADS box of SOC1 causes loss of binding to the *LFY* promoter as well as suppression of the flowering promotion function. The full-length SOC1 protein locates in the cytoplasm if expressed alone in protoplast transient expression assay, but relocates to the nucleus if expressed with AGAMOUS-LIKE 24 (AGL24), another flowering pathway integrator and a MADS box protein. The domain analysis shows that co-localization of SOC1 and AGL24 is mediated by the MADS box and the intervening region of SOC1. Finally, we show that *LFY* is expressed only in those tissues where *SOC1* and *AGL24* expressions overlap. Thus, we propose that heterodimerization of SOC1 and AGL24 is a key mechanism in activating *LFY* expression.**

Keywords: ***SOC1, AGL24, LFY,* heterodimerization, nuclear translocation, flowering time.**

Introduction

The proper timing of flowering at a specific season is critical for plant survival; thus plants have evolved a sophisticated mechanism to control flowering in response to both environmental factors and endogenous signals. Extensive genetic analyses of Arabidopsis have revealed that three genes, the so-called flowering pathway integrators *FT*, *SUPPRESSOR OF OVEREXPRESSION OF CONSTANS1* (*SOC1*) and *LEAFY* (*LFY*), integrate signals from multiple flowering pathways; thus, the expression levels of these three genes eventually determine the exact flowering time (Amasino, 2005; Hayama and Coupland, 2003; Parcy, 2005; Simpson and Dean, 2002; Sung *et al.*, 2003).

The *SOC1* gene has been identified by three independent approaches (Lee *et al.*, 2000; Onouchi *et al.*, 2000; Samach *et al.*, 2000). It has been identified through a screening of loss-of-function suppressor mutants from overexpressor of *CONSTANS* (*CO*), a plant line exhibiting an extremely early flowering phenotype (Onouchi *et al.*, 2000). This indicates that *SOC1* is a downstream target of CO, which is a central regulator of the photoperiod pathway (Hayama and Coupland, 2003). Indeed, *SOC1* has been isolated as a direct target of CO (Samach *et al.*, 2000). It has also been identified through the screening of gain-of-function suppressor mutants from extremely late flowering winter annual plants that have both *FRIGIDA* (*FRI*) and *FLOWERING LOCUS C* (*FLC*): the suppressor mutant with activation tagging of *SOC1* showed overexpression of *SOC1* and suppression of the late flowering phenotype caused by high expression of *FLC* in winter annuals or autonomous pathway mutants (Lee *et al.*, 2000). This indicates that SOC1 is a downstream target of *FLC*. It has also been shown that FLC regulates expression of *SOC1* by direct binding to the promoter (Hepworth *et al.*, 2002). The *soc1-2* loss-of-function mutant exhibits a late-flowering phenotype and has decreased *LFY* expression, whereas the *soc1-101D* gain-of-function mutant exhibits an extremely early flowering phenotype and has increased *LFY*

expression, thus indicating that SOC1 acts upstream of *LFY* (Moon *et al.*, 2003, 2005). However, the mechanism by which SOC1 regulates *LFY* has not been elucidated yet.

Both *SOC1* and *FLC* encode a MADS box transcription factor. Another MADS box gene, *AGAMOUS-LIKE 24* (*AGL24*), has recently been proposed as a flowering pathway integrator (Michaels *et al.*, 2003; Yu *et al.*, 2002). Expression of *AGL24* is regulated by multiple flowering pathways such as the photoperiod pathway, the autonomous pathway and vernalization. Similar to *soc1*, *LFY* expression is reduced in *agl24* (Yu *et al.*, 2002). Interestingly, *SOC1* and *AGL24* show largely overlapping expression in the shoot apex at the moment of floral transition. In addition, overexpression of one gene has little effect on the flowering of the mutant in the other gene (Michaels *et al.*, 2003), suggesting that SOC1 and AGL24 act together as a complex protein. However, this hypothesis has not been tested empirically.

The proteins SOC1, AGL24 and FLC are all MIKC type MADS box proteins composed of four characteristic domains: the MADS box (M), an intervening (I) region, a keratin (K) box and a C-terminal domain from the N-terminus to the C-terminus (Riechmann and Meyerowitz, 1997a,b). MADS box proteins in angiosperms have functions regulating diverse developmental processes such as control of flowering time, floral meristem identity, floral organ development and fruit development (Alvarez-Buylla *et al.*, 2000; Arabidopsis Genome Initiative, 2000; Riechmann and Ratcliffe, 2000; Theissen *et al.*, 2000). The MADS domain, composed of 56–58 amino acids, is the most highly conserved domain, and has functions in DNA binding and dimerization, as demonstrated by X-ray crystallographic analyses of MADS proteins such as human serum response factor (SRF), human myosin enhancer factor 2A (MEF2A) and the yeast mating type determining factor MCM1 (Han *et al.*, 2003; Pellegrini *et al.*, 1995; Santelli and Richmond, 2000; Tan and Richmond, 1998). The crystal structure reveals that the N-terminus of the MADS box, including an N-extension and an α-helix (amino acid residues 23–31), provides the primary DNA-binding contacts over the consensus-binding sequence whereas the C-terminus of the MADS box, containing two anti-parallel β-sheets, functions as a dimerization interface (de Folter and Angenent, 2006). Consistently, the introduction of missense mutation in the MADS domain causes a developmental defect in rice flowers, indicating the functional significance of the MADS box (Jeon *et al.*, 2000). The conserved K domain provides the coiled-coil structure with amphipathic α-helices, probably involved in protein–protein interaction (Riechmann and Meyerowitz, 1997b). It has been suggested that the K domain is required for heterodimerization of the MADS box proteins involved in floral organ identity (Fan *et al.*, 1997; Yang *et al.*, 2003). The I region is inserted between the MADS and K domains. Domain swapping analyses between organ identity genes such as *APETALA3* (*AP3*), *PISTILLATA* (*PI*), *AGAMOUS* (*AG*) and *APETALA1* (*AP1*) revealed that the I domain is necessary for the dimerization and functional specificity of each MADS protein (Krizek and Meyerowitz, 1996; Riechmann and Meyerowitz, 1997a; Riechmann *et al.*, 1996a). The C-terminal domain is the most variable domain, in both length and sequence. In some MADS proteins, the C domain possesses transcriptional activation activity (Cho *et al.*, 1999; Honma and Goto, 2001). In other cases it is required to form multimeric complexes among MADS proteins (Egea-Cortines *et al.*, 1999; Honma and Goto, 2001).

In this study, we analyzed how the SOC1 protein regulates *LFY* expression. An *in vivo* chromatin immunoprecipitation assay showed that SOC1 directly binds to the *LFY* promoter, and the missense mutation in the MADS box causes both complete suppression of *SOC1* function and loss of binding to the *LFY* promoter. Transient expression assay showed that full-length SOC1 is localized in the nucleus but the interaction with AGL24 relocates the dimer to the nucleus. Therefore, our results provide empirical evidence showing that the interaction of SOC1 and AGL24 is required for activation of *LFY*.

Results

Analysis of intragenic suppressor mutants of soc1-101D FRI

soc1-101D FRI, an overexpressor of *SOC1*, has been isolated as an early flowering mutant suppressing the very late flowering phenotype of winter annual Arabidopsis strains, *FRIGIDA* containing Columbia (*FRI*-Col) (Lee *et al.*, 2000). To analyze the SOC1 protein biochemically, we screened intragenic suppressor mutants of *soc1-101D FRI*. We performed ethylmethane sulfonate (EMS) mutagenesis and isolated the mutants showing a late-flowering phenotype, which we named *sso* (*suppressor of soc1-101D FRI*). A total of 17 mutants that showed stable transmission to subsequent generations were isolated. To distinguish intragenic and intergenic suppressors, we crossed the mutants with *FRI*-Col plants. We expected that the F_1 progeny from the cross with intragenic suppressors would flower very late, whereas those crossed with intergenic suppressors would flower as early as the *soc1-101D FRI* heterozygote. Among the 17 *sso* mutants, 11 mutants produced F_1 progeny flowering as late as *FRI*-Col. To confirm whether they were indeed intragenic suppressors, we sequenced the coding region of *SOC1* in individual mutants after PCR amplification (Figure 1). All of the 11 mutants showed intragenic mutation: nine G to A transitions, one C to T transition and one 28-bp deletion in the *SOC1* coding sequence. Interestingly, *sso11*, *-12*, *-13* and *-52* have the same mutation in MADS box and *sso1*, *-2* and *-51* have the same mutation in the I domain. The mutations were found in MADS, I and K domains but not in the C domain (Figure 1a, c).

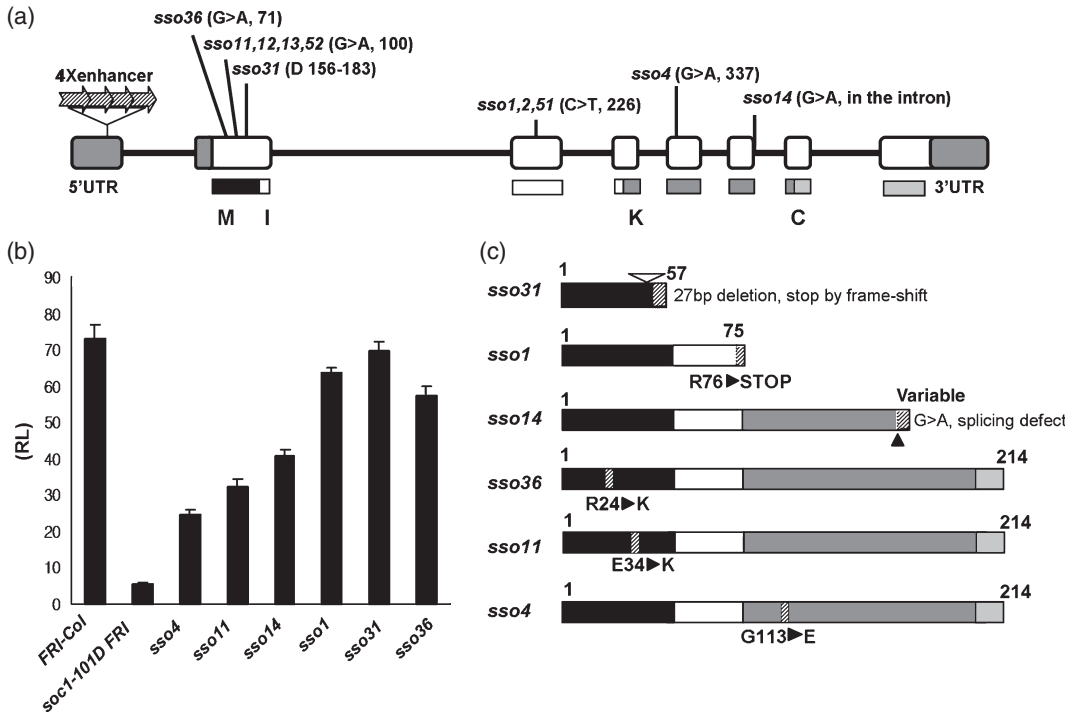

Figure 1. Analysis of intragenic suppressor mutants in *soc1-101D FRI*.
(a) Overview of *sso* mutations on a schematic diagram of the *SOC1* gene. The *SOC1* gene has eight exons and seven introns with 5′ and 3′ untranslated regions (UTR). The eleven mutants obtained by EMS mutagenesis show six different mutation events.
(b) Flowering time of six *sso* mutants. Flowering time was measured from more than 20 plants from each line grown in long days.
(c) Schematic structures of SOC1 mutant proteins. Four characteristic domains of SOC1 are depicted with black (MADS), white (I), dark gray (K) and light gray (C) bars.

The flowering phenotype of intragenic suppressors was found to be dependent on the type of mutation (Figure 1b, c). The *sso31* and *sso1* mutants showed the strongest and almost complete suppression of the early flowering phenotype in *soc1-101D FRI*. The *sso31* mutation caused a 28-bp deletion at the end of the MADS domain, thus producing a partial fragment of SOC1 with only the MADS domain, due to frameshifting. The *sso1* caused nonsense mutation in the middle of the I domain, thus producing a partial fragment of SOC1 with MADS and part of the I domain. The *sso14* mutation caused a donor site mutation in the sixth intron, thus producing proteins with the deletion in part of the K and C domains. The *sso14* mutant showed relatively weaker suppression, which indicates that the truncated SOC1 protein has partial activity. In general, the missense mutations caused weak suppression (Figure 1b, c). The *sso11* mutant has a missense mutation in the MADS domain changing Glu34 to Lys, and the *sso4* mutant has a missense mutation in the K domain changing Gly113 to Glu. Both of the mutants showed relatively weak suppression, although the flowering is significantly delayed compared with *soc1-101D FRI*. In contrast to these mutants, the missense mutation in *sso36*, changing Arg24 to Lys, caused a strong suppression (Figure 1b, c), which suggests that Arg24 is highly critical for the function of SOC1. Indeed, previous X-ray crystallographic analysis of MADS box proteins showed that Arg24 binds directly to the phosphate backbone of DNA in the minor groove (Pellegrini *et al.*, 1995; Santelli and Richmond, 2000; Tan and Richmond, 1998). Therefore, our result supports the view that the SOC1 protein binds to the promoter of target genes through Arg24. Our result also suggests that Glu34 in the MADS domain is important for the functioning of SOC1.

SOC1 directly binds to the LFY *promoter*

It has been suggested that SOC1 acts upstream of *LFY* (Lee *et al.*, 2000; Moon *et al.*, 2003, 2005; Samach *et al.*, 2000). However, it has not yet been proven whether SOC1 regulates *LFY* directly. To test this, we performed chromatin immunoprecipitation (ChIP) using *soc1-2* (loss-of-function mutant) and *soc1-101D* (gain-of-function mutant) with anti-SOC1 antibody (Figure 2). The wild type was not used in this analysis because we failed to detect the SOC1 protein by any method, probably due to there being too small an amount. To define the binding sequences, the 2.2-kb *LFY* promoter was divided into eight overlapping segments (a–h), from distal to proximal regions from the ATG start codon (Figure 2B). The result showed that the regions of the distal segments a and b and the proximal segments g and h, where

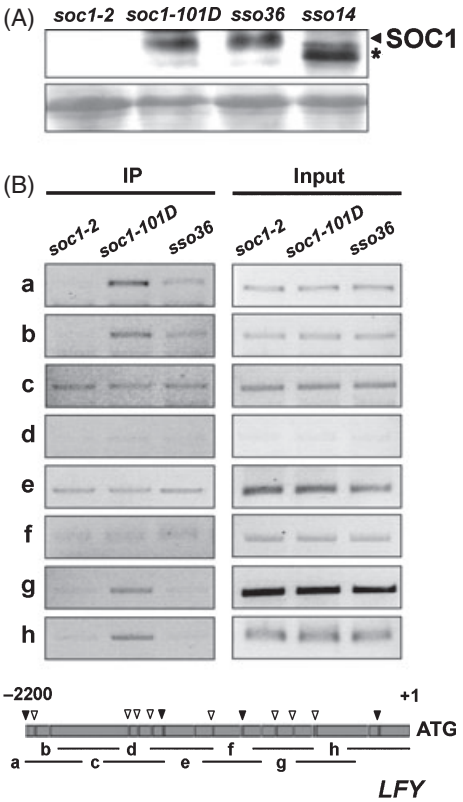

Figure 2. Analysis of binding of SOC1 to the *LFY* promoter.
(A) Western blot analysis with anti-SOC1 antibody in *soc1-2, soc1-101D FRI, sso36* and *sso14*. The level of SOC1 protein is not significantly changed by *sso36* mutation. The mutant *sso14* shows the reduced size of the SOC1 truncated protein (*). Below is the Ponceau staining as a loading control.
(B) Chromatin immunoprecipitation (ChIP) assay with SOC1 antibody for the *LFY* promoter. The SOC1 binds to the distal regions (a and b) and proximal regions (g and h). In contrast, *sso36* mutation causes reduced binding to the same regions. The chromatins were extracted from 9-day-old seedlings. The graphic bar below represents the full-length 2.2-kb *LFY* promoter. The arrowheads denote putative CArG boxes (open, variant form). For quantitative controls, input DNA was extracted from resuspended nuclear extracts, and 1 μl of 1/200 diluted input DNA was used in a PCR reaction.

variant forms of the CArG box are present, are enriched in *soc1-101D* compared with *soc1-2* by ChIP (Figure 2B). The same result was obtained from ChIP analysis of *35S-SOC1:-MYC* using anti-Myc antibody (data not shown). In contrast, *sso36* mutants, which have a mutation in Arg24, showed significantly reduced enrichment in segments a and b and no enrichment in segments g and h. This again supports the view that the Arg24 in SOC1 is required for physical contact with the target gene, *LFY*. Taken together, our *in vivo* binding analysis shows that SOC1 directly binds to the *LFY* promoter.

SOC1 is translocated to the nucleus by interaction with AGL24

Since nuclear localization of many MADS box proteins is regulated by heterodimerization (Ferrario *et al.*, 2004; Immink and Angenent, 2002; McGonigle *et al.*, 1996), we wondered if SOC1 protein localization is also regulated. The subcellular localization was determined by Arabidopsis protoplast transfection assay using a fusion construct of full-length SOC1 with a green fluorescent protein (*SOC1:GFP*). As shown in Figure 3, the SOC1 protein was not detected in the nucleus but instead localized in the cytosol as large speckles. To confirm this, we further examined whether the SOC1 protein is detected in cytoplasmic fractions in *35S-SOC1:MYC* transgenic plants by Western blotting (Figure 3i). The SOC1:MYC fusion protein was detected at much higher levels in cytoplasmic fractions than nuclear fractions in shoot apex and leaves where the *SOC1* promotes flowering (Searle *et al.*, 2006). However, in the root, the level of SOC1:MYC protein was similar in both cytoplasmic and nuclear fractions. The subcellular localization of SOC1:GFP fusion protein in *35S-SOC1:GFP* transgenic plants, which complement the *soc1-2* mutant, further confirmed this result (Figure S1). The SOC1:GFP fusion protein was found to be widespread in the root cells of *35S-SOC1:GFP* transgenic plants, indicating that most of the biologically active SOC1:GFP protein remains in the cytosol.

Because genetic interaction between *SOC1* and *AGL24* and the SOC1–AGL24 protein interaction have been reported using yeast two hybrid analysis (de Folter *et al.*, 2005; Michaels *et al.*, 2003; Yu *et al.*, 2002), we checked if SOC1–AGL24 interaction affects the subcellular localization of SOC1. First, the subcellular localization of AGL24 was determined by Arabidopsis protoplast transfection assay using *AGL24:RFP* (Figure 3). The fluorescence of red fluorescent protein (RFP) was only detected in the nucleus, suggesting that AGL24 is constitutively localized in the nucleus. In contrast, if both *SOC1:GFP* and *AGL24:RFP* were introduced into protoplast, the SOC1 and AGL24 proteins were co-localized in the nucleus. These results suggest that translocation of SOC1 to the nucleus requires interaction with AGL24.

The MADS and I domains of SOC1 are required to interact with AGL24

To elucidate which domain mediates the heterodimerization between SOC1 and AGL24, a series of truncated SOC1 proteins fused to GFP were constructed and transfected into protoplasts, as indicated in Figure 4(A). When introduced alone, $SOC1_M$ and $SOC1_{MI}$ truncated proteins were localized in the nucleus (Figure 4C, D), suggesting that the MADS domain is necessary for the nuclear localization of SOC1. Consistently, $SOC1_{IKC}$ and $SOC1_{KC}$ were mainly localized in the cytoplasm due to the lack of a MADS domain (Figure 4E, F). It is also noteworthy that the exact cytoplasmic localization of $SOC1_{IKC}$ and $SOC1_{KC}$ is different from that of full-length SOC1 (compare Figure 4E, F and 3a). This result suggests two things. Firstly, the K and C domains prevent

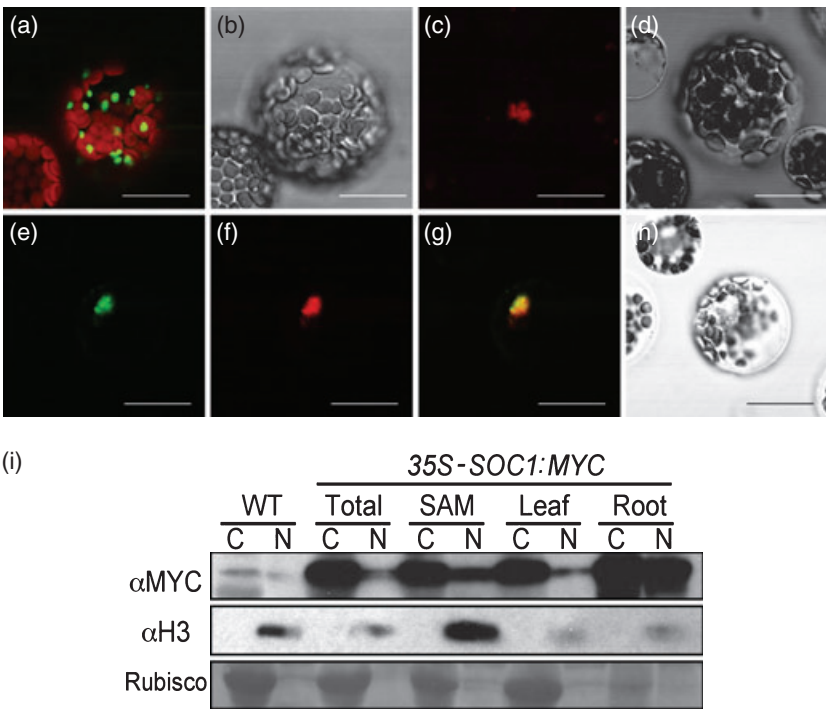

Figure 3. Subcellular localization of SOC1 and AGL24.
(a) The SOC1:GFP fusion proteins are localized in the cytoplasm as large speckles. The red signal is from the autofluorescence of chloroplasts.
(b) Bright field image of SOC1:GFP.
(c) The AGL24:RFP fusion proteins are mainly localized in the nucleus.
(d) Bright field image of AGL24:RFP.
(e)–(h) Protoplast cells expressing SOC1:GFP and AGL24:RFP simultaneously. (e), (f) Protoplasts imaged with GFP and RFP filters, respectively. (g) Merge of (e) and (f). (h) Bright field image of SOC1:GFP and AGL24:RFP co-transfection. The scale bars at the bottom represent 20 μm.
(i) Subcellular localization of SOC1 proteins in transgenic *35S::SOC1-MYC*. SOC1:MYC proteins are abundant in the cytoplasmic fractions. Proteins were extracted from the whole seedlings (Total), shoot apical meristem (SAM), young leaves (Leaf), roots (Root), and subdivided into the nuclear (N) and cytoplasmic (C) fractions. Anti-MYC antibody was used to detect SOC1:MYC proteins. The purity of each fraction was demonstrated by anti-histone 3 antibody, and Ponceau staining of Rubisco protein. For reference, 5% and 100% of the total amount of extracts are loaded for cytoplasmic and nuclear fractions, respectively.

SOC1 from being translocated to the nucleus. Secondly, the MADS domain also affects the subcellular localization of the K and C domains, thus transporting SOC1 to a unique cytoplasmic region.

When the truncated forms of SOC1 were expressed together with AGL24:RFP, all the proteins except $SOC1_{KC}$ showed perfect co-localization with AGL24 in the nucleus (Figure 4B–F). In contrast, the $SOC1_{KC}$ protein could no longer be imported into the nucleus with AGL24 (Figure 4F). These findings suggest that the MADS and I domains of SOC1 are required not only for nuclear localization but also for heterodimerization with AGL24.

AGL24 directly binds to the LFY *promoter and acts with SOC1*

Since our results indicate that AGL24 interacts with SOC1, and that heterodimerization is required for the nuclear transport of SOC1, it is expected that AGL24 should bind to the same region of the *LFY* promoter where SOC1 binds. To test this hypothesis, we performed ChIP using *35S-AGL24:-HA* with the same sets of primers used as shown in Figure 2. As is shown in Figure 5(A), the distal segments a and b and the proximal segments f and g of the *LFY* promoter were relatively enriched. These regions are well correlated with the regions bound by SOC1.

If SOC1 and AGL24 act together to regulate *LFY*, it is expected that the expression regions of the two genes overlap. Although the tissue specificity of the two genes has been reported previously (Lee *et al.*, 2000; Samach *et al.*, 2000; Yu *et al.*, 2002, 2004), we re-examined the expression with that of *LFY* in the same tissue samples (Figure 5B). We collected young leaves, shoot apices and roots separately from 9-day-old seedlings, and stems and inflorescences separately from 30-day-old adult plants. The result showed that *SOC1* is widely expressed, from roots to leaves, stems, shoots and inflorescence, whereas *AGL24* is expressed in shoots, stems and inflorescence but is not expressed in the roots and young leaves. Interestingly, *LFY* is expressed only in the region where *SOC1* and *AGL24* expressions overlap, which supports our hypothesis that the interaction of SOC1 and AGL24 is necessary for *LFY* regulation. However, it is

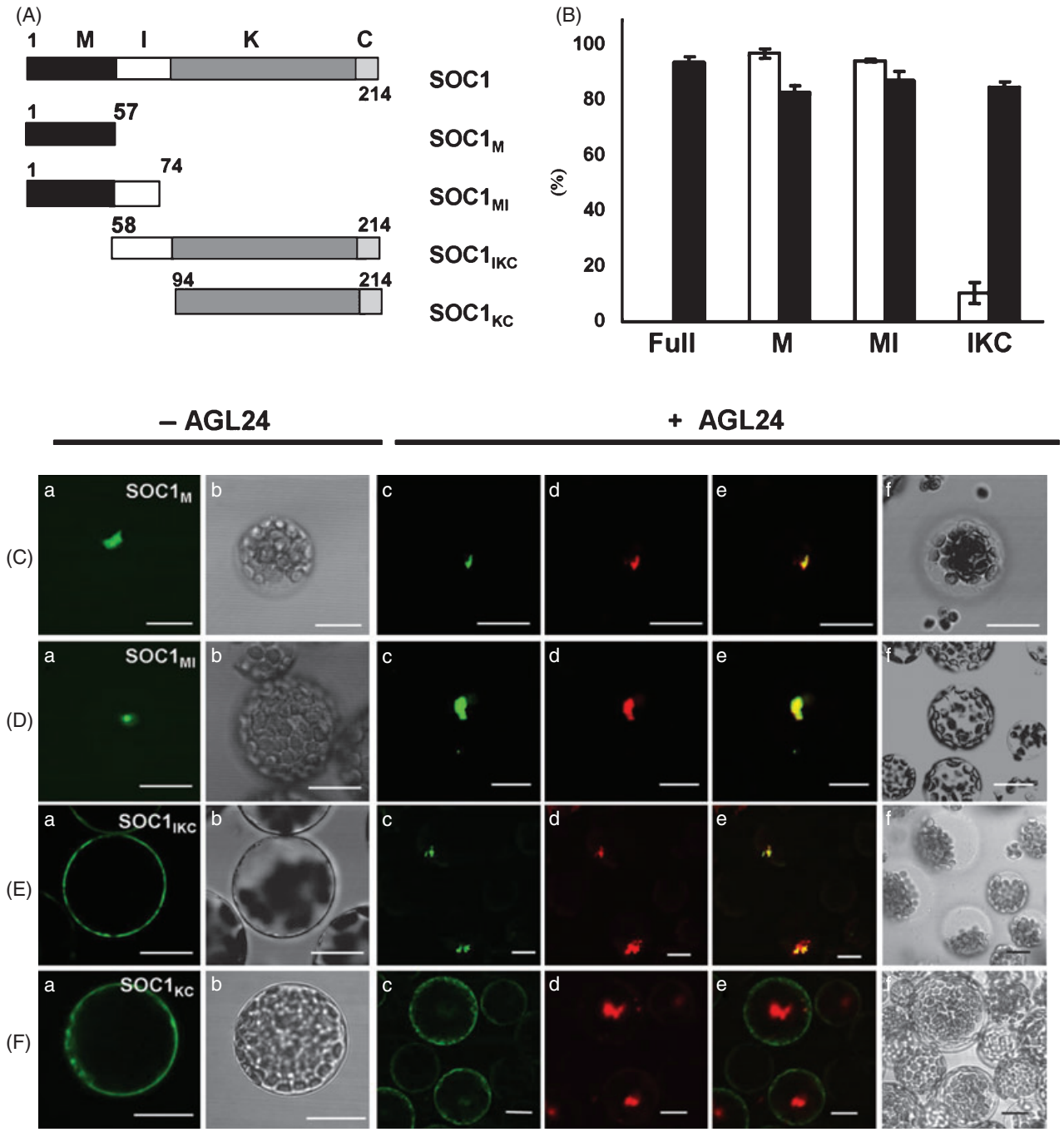

Figure 4. Confocal laser scanning microscopy of Arabidopsis protoplasts expressing truncated series of SOC1:GFP and AGL24:RFP.
(A) Schematic representation of full-length SOC1 protein. The location of amino acids at the start and end points of the coding regions in constructs are marked as numbers.
(B) The percentage of nuclear localization of the GFP signal observed for truncated series of SOC1:GFP with (black bars) and without AGL24:RFP (white bars).
(C)–(F) Protoplasts expressing a series of truncated SOC1:GFP fusion proteins (a, b) and protoplasts co-expressing truncated SOC1:GFP and full-length AGL24:RFP. Protoplasts were imaged with GFP filters (c) and RFP filters (d), respectively. Merged images (e) and bright field images (b–f) are shown together. The scale bars at the bottom represent 20 μm.

noteworthy that *LFY* is not expressed in the stems where SOC1 and AGL24 expressions overlap. This suggests that the interaction of SOC1 and AGL24 is necessary but not sufficient to activate *LFY*.

Discussion

It has long been perceived that the floral meristem identity gene, *LFY*, links floral induction and floral development

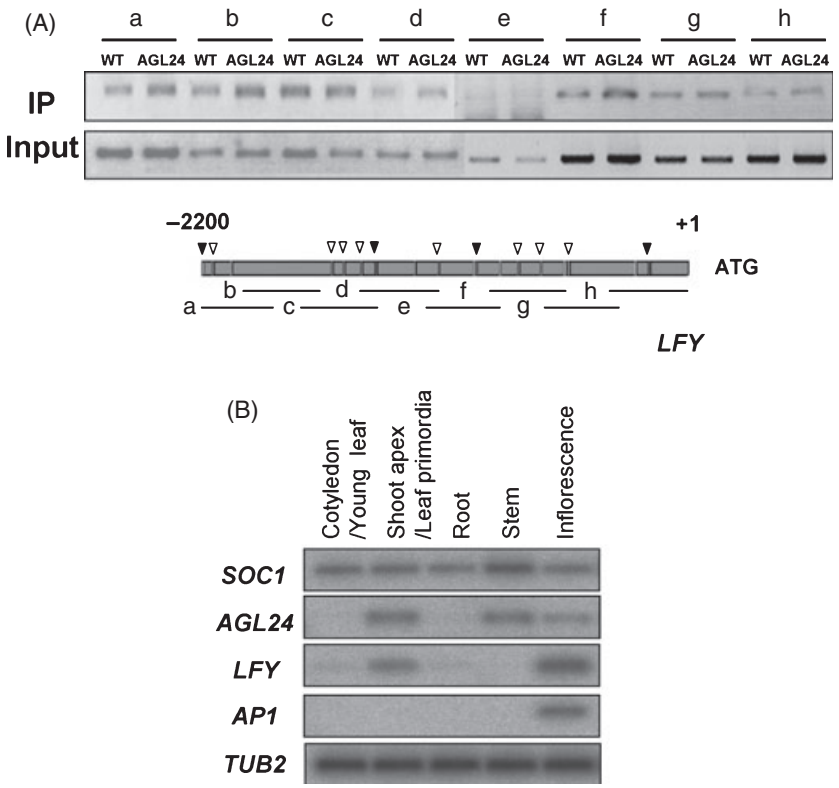

Figure 5. Analysis of AGL24 binding to the *LFY* promoter and tissue-specific expression of *SOC1*, *AGL24* and *LFY*.
(A) Chromatin immunoprecipitation (ChIP) assay for the *LFY* promoter in wild type (WT) and *35S-AGL24:6HA* with HA antibody and the same sets of primers as used in Figure 2. The regions a, b, f and g on the *LFY* promoter showed significant enrichment in *35S-AGL24:6HA*.
(B) Tissue-specific expression of *SOC1*, *AGL24* and *LFY* in WT was determined by RT-PCR. Total RNAs of young leaf/cotyledon, shoot apices/leaf primordia and root tissues were extracted from 9-day-old seedlings. *SOC1* is ubiquitously expressed in various tissues and transcripts of *AGL24* and *LFY* are mainly detected in the shoot apex in 9-day-old seedlings. Total RNAs of stems, inflorescences and rosette leaves were extracted from adult plants. All tissues were harvested 12 h after dawn.

(Blazquez and Weigel, 2000; Parcy, 2005). However, the molecular mechanism by which *LFY* links the two developmental processes has not been completely understood. Here, we show that a flowering pathway integrator, SOC1, directly binds to the *LFY* promoter harboring variant forms of the CArG box, and that nuclear localization of SOC1 requires interaction with another flowering pathway integrator AGL24 through MADS domain-mediated heterodimerization. In addition, we show that *LFY* is expressed only in the domain where *SOC1* and *AGL24* expressions overlap. Taken together, we propose that the heterodimerization of SOC1 and AGL24 is a key mechanism in the activation of *LFY* expression.

Many plant MADS domain proteins bind *in vitro* to the CArG box sequence as either homodimers or heterodimers. Binding to a DNA sequence containing the CArG box motif has been shown for the Arabidopsis MADS domain proteins AGAMOUS (AG), APETALA1 (AP1), APETALA3 (AP3), PISTILLATA (PI), AGAMOUS LIKE 15 (AGL15), FLC and SHORT VEGETATIVE PHASE (SVP) (Hepworth *et al.*, 2002; Huang *et al.*, 1993; Lee *et al.*, 2007a,b; Riechmann *et al.*, 1996b; Shiraishi *et al.*, 1993). These studies revealed that plant MADS domain proteins bind to a CArG box with the core sequence (CCW_6GG) in either *in vitro* or *in vivo* binding assays. Recent studies have shown that binding also occurs to a variant form of consensus sequence depending on the proteins tested and that the nucleotides outside the core sequence also contribute to the recognition site for binding, reflecting the specificity of the plant MADS domain family for particular target sites (de Folter and Angenent, 2006). Several variants of the CArG box are found across the *LFY* promoter (shown in Figure 2). Our ChIP analysis showed that both SOC1 and AGL24 bind *in vivo* to the proximal and distal regions in the *LFY* promoter where variant forms of the CArG box are present. Consistent with this, previous analysis of the *LFY* promoter showed that the deletion in the distal region (regions a and b in Figure 2) caused a significant decrease in promoter strength, and that the proximal region (regions g and h) contains a gibberellin-responsive *cis*-element for flowering regulation (Blazquez and Weigel, 2000).

The analysis of intragenic suppressor mutations in *soc1-101D FRI* further supports our proposal that SOC1 directly regulates *LFY* expression. The strongest suppression among missense mutations is observed in the mutant replacing Arg24 with Lys. The missense mutations in Glu34 and Gly113 also cause apparent suppression of SOC1 function. Amino acid sequence alignment among MIKC-type MADS box proteins showed that Arg24 is completely conserved in all the MADS proteins. Glutamic acid-34 and Gly113 also are very highly conserved among MADS proteins (Figure S2). Interestingly, Glu34 is replaced with Gln in *FLC* clade genes which have the opposite function in flowering time regulation with SOC1 and AGL24. X-ray crystallographic analysis of MADS box proteins, such as human SRF, MEF2 and yeast MCM1, has shown that Lys23 and Arg24 directly bind to the

phosphate group of DNA in major and minor grooves, respectively, and that Glu34 hydrogen bonds to Arg24 from its dimerization partner protein, which is critical for specifying the local DNA conformation (Pellegrini *et al.*, 1995; Santelli and Richmond, 2000; Tan and Richmond, 1998). Consistent with these structural analyses, the missense mutation of Arg24 to Lys in *sso36* resulted in the loss of binding to the proximal and distal regions of the *LFY* promoter (Figure 2). Therefore, our result confirms that SOC1 protein binds to the *LFY* promoter through Arg24, helped by Glu34.

When the full-length SOC1 protein is overexpressed alone, it is mainly localized in the cytoplasm in both the protoplast transient assay and stable transformant plants (Figure 3). The protoplast transient assay, using constructs of GFP fusion with truncated SOC1 protein, indicated that the MADS domain has an ability to localize in the nucleus but the K and C domains somehow mask the nuclear localization signals (NLS) in the MADS domain. However, if the full-length SOC1 protein is co-expressed with AGL24, the two proteins co-localize in the nucleus. It is possible that heterodimerization with AGL24 causes a conformational change in SOC1, thus exposing the NLS located in the MADS domain. Additionally, since AGL24 alone localizes in the nucleus, the NLS in AGL24 may be sufficient for the translocation of the AGL24–SOC1 heterodimer to the nucleus. Indeed, $SOC1_{IKC}$, which shows interaction with AGL24 due to the I domain, co-translocated with AGL24 to the nucleus, although it lacks the MADS domain from SOC1 (Figure 4E).

Such relocations, from cytoplasm to nucleus of MADS proteins by heterodimerization, have been reported in AP3, PI and the petunia SOC1 homolog, UNSHAVEN (UNS) protein (Ferrario *et al.*, 2004; McGonigle *et al.*, 1996). In the case of AP3 and PI, the heterodimerization of the two proteins resulted in relocation to the nucleus, and the co-localization signals were mapped onto the MADS domain. Similarly, in the case of UNS, heterodimerization with another petunia MADS box protein, FBP9, caused translocation to the nucleus. However, the UNS deleted with MADS plus I domains successfully interacts with FBP9 and co-localizes with FBP9 in the cytoplasm, indicating that heterodimerization and nuclear translocation are independent mechanisms. In contrast, the SOC1 protein deleted with MADS plus I domains failed to co-localize with AGL24 (Figure 4F). Thus, translocation of SOC1 seems to depend on the MADS and I domains that are required for both heterodimerization with AGL24 and nuclear translocation, which is more similar to AP3–PI interaction. The protein products from *soc1-101D* suppressor mutants with missense mutations showed normal co-localization to the nucleus with AGL24 (Figure S3), suggesting that the mutant phenotype was caused not by failure of heterodimerization with AGL24 but by failure to bind to the DNA in the target gene.

Because the previous interactome analysis of Arabidopsis MADS box protein showed that SOC1 protein interacts not only with AGL24 but also with SVP, which is the closest homolog to AGL24 in protein sequence but has an opposite flowering effect (de Folter *et al.*, 2005), we checked whether SOC1 localization is also affected by co-expression of SVP in transient assay. Interestingly, SOC1 was also translocated to the nucleus by SVP (JG, MO, HP, IL, unpublished results). This suggests that SVP and AGL24 may act as floral repressor and inducer, respectively, through competitive dimerization with the same binding partner, SOC1. Alternatively, both AGL24–SOC1 and SVP–SOC1 dimers have a common function other than flowering time regulation, such as maintenance of inflorescence identity, because it has been suggested that SOC1, AGL24, SVP have a function in inflorescence identity (Gregis *et al.*, 2006; Liu *et al.*, 2007; Yu *et al.*, 2004). Further analysis is required to elucidate the functional significance of the SOC1–SVP complex.

The interactome analysis of the Arabidopsis MADS box protein also showed that SOC1 protein not only interacts with flowering time genes, *AGL24* and *SVP*, but also with the floral homeotic genes, *AP1*, *FUL* and *SEP1*, *-2*, *-3*; thus, positive and negative feedback loops have been proposed (de Folter *et al.*, 2005). The SOC1–AGL24 interaction results obtained in this study substantiate such a hypothesis. Our results indicate that the spatial and temporal co-expression of the two genes is critical for the formation of a functional complex, and indeed the expression domain of the two genes overlap where the target gene, *LFY*, is expressed. Taken together with our results and the previous reports, we propose a model of the regulatory mechanism of *LFY* by SOC1 and AGL24 (Figure 6). *SOC1* is induced in whole tissues including shoot apices and leaves; however, in the leaves, SOC1 is mainly located in the cytoplasm in the absence of binding partners, and thus cannot induce *LFY*. As *AGL24* is induced in shoot apical meristem, the cells that express SOC1 and AGL24 simultaneously have an active nuclear MADS protein complex inducing *LFY* expression. However, SOC1 and AGL24 interaction seems insufficient to induce *LFY* because *LFY* expression is constrained in the emerging leaf primordia and anlagen, although the expressions of SOC1 and AGL24 largely overlap throughout the shoot apical meristem (Figure 6). Thus, some other factors may be required for induction of *LFY* in emerging primordia. Alternatively, TERMINAL FLOWER 1 (TFL1), an antagonist of LFY activity, may repress the activity of the SOC1–AGL24 complex. The TFL1 protein locates in the outer layers of shoot apical meristem where AGL24 is expressed, and represses the *LFY* gene in the central domain of the shoot apical meristem (Conti and Bradley, 2007). With such strict control by flowering regulators, *LFY* starts to be activated in floral anlagen (Figure 6). Eventually, as the floral meristem develops, AP1, induced by LFY, represses the expression of SOC1 and AGL24 in the inflorescence, as reported (Yu *et al.*, 2004).

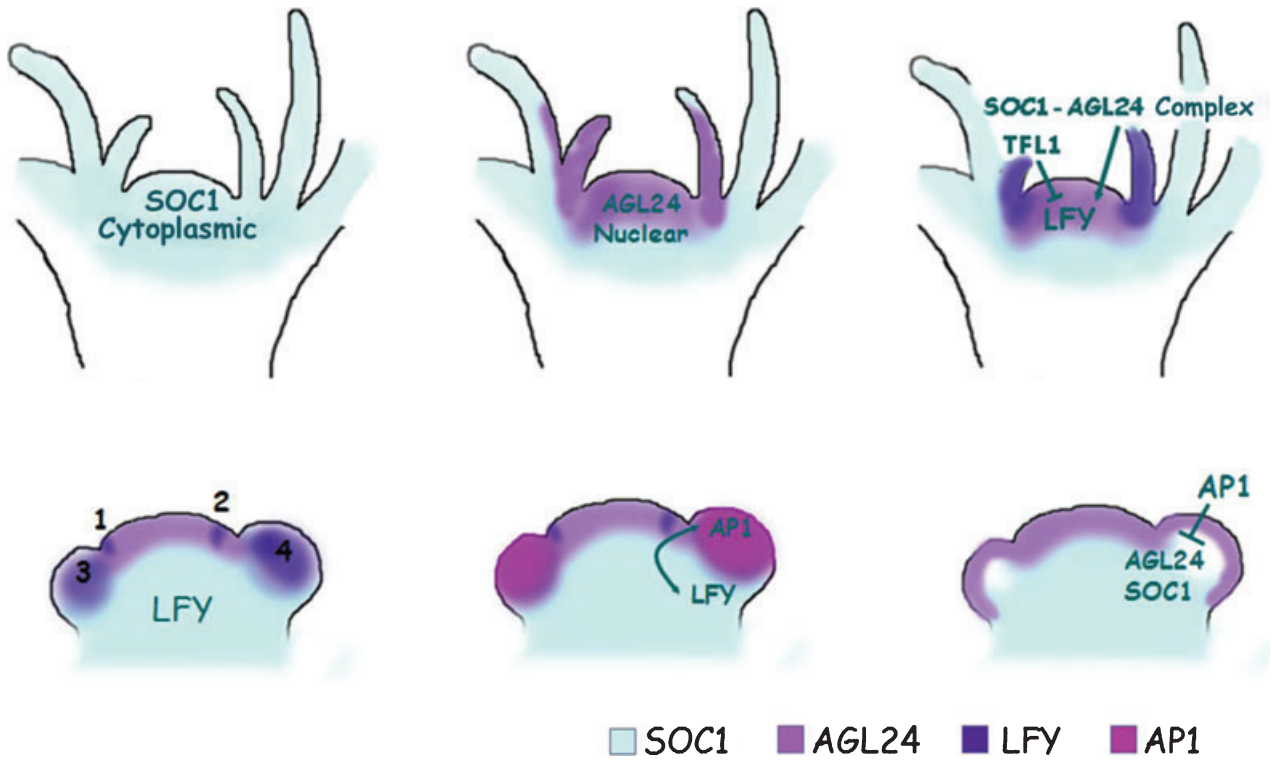

Figure 6. The model of regulation of *LFY* by the interaction of SOC1 and AGL24.
SOC1 is induced in various tissues from early developmental stages. As *AGL24* is induced in shoot apical meristem, SOC1 and AGL24 can make active nuclear MADS protein complex, inducing *LFY* expression. In the central domain of the shoot apical meristem, TFL1, which strongly restricts *LFY* expression, acts antagonistically to the SOC1:AGL24 complex. Such a precise control by flowering regulators restricts activation of *LFY* confined in floral anlagen and eventually in the whole floral meristem. As the floral meristem develops, AP1 is induced and represses the expression of SOC1 and AGL24 in the inflorescence.

Experimental procedures

Plant materials and growth conditions

Arabidopsis thaliana ecotype Columbia was used as the wild type. The seeds were stratified on 0.8% phytoagar containing half-strength Murashige and Skoog (Plantmedia, http://www.plantmedia.com/) salts for 3 days at 4°C. Afterwards, the plants were grown in long days (16-h light/8-h dark) under cool white fluorescent lights (100 μmol m^{-2} sec^{-1}) at 22°C. For all the experiments, tissues were harvested at 12 h after lights on. To screen suppressor mutations of *soc1-101D FRI* (Lee *et al.*, 2000), 30 000 M_0 seeds were mutagenized with ethyl methanesulfonate (EMS). Individuals that flowered later than the *soc1-101D FRI* were identified in an M_2 population of approximately 30 000 plants representing ~8000 M_1 plants after mutagenesis.

Plasmid construction

To generate the transgenic plants expressing MYC-tagged SOC1, we used pC-TAP vector described previously (Rubio *et al.*, 2005). The coding region of SOC1 was PCR-amplified using the *att*B sequence containing primers (forward primer 5′-AGG CTA TAC AAA ATG GTG AGG GGC AAA ACT CAG A-3′; reverse primer 5′-GAA AGC TGG GTA TCC CTT TCT TGA AGA ACA AGG-3′), cloned into the pDONR 201 plasmid using the BP reaction (Gateway; Invitrogen, http://www.invitrogen.com/). After checking the DNA sequence, the SOC1 coding region was transferred from the pDONR 201 to the pC-TAPa vector using the LR reaction (Gateway; Invitrogen). The resulting constructs were introduced to L*er* by *Agrobacterium-tumefaciens* mediated transformation. The transgenic plants showing earlier flowering than wild type were chosen for further analysis. The *35S-AGL24:6HA* was kindly provided by Dr H. Yu (National University of Singapore, Singapore).

For construction of a gene encoding a GFP fusion, a PCR fragment containing the coding region of *SOC1* without a stop codon was amplified with forward primer (L11: 5′-GCT CTA GAG CAT GGT GAG GGG CAA AA-3′) and reverse primer (L21: 5′-CGG GAT CCA CTT TCT TGA AGA ACA AGG T-3′). The fragment was inserted at the *Xba*I and *Bam*HI restriction sites of the p326-GFP vector (Lee *et al.*, 2001). The GFP fusions of $SOC1_M$, $SOC1_{MI}$, $SOC1_{IKC}$, $SOC1_{KC}$, SSO1, SSO4, SSO11, SSO14, SSO31 and SSO36 were cloned using a similar strategy. The primers for PCR amplification were: for $SOC1_M$ (L11 and reverse primer L22: CGG GAT CCA GAA TTC ATA AAG TTT), for SOC_{MI} (SSO1) (L11 and reverse primer L23: CGG GAT CCA ATC CTT AGT ATG CCT C), for $SOC1_{IKC}$ (forward primer L12: GCT CTA GAG CGC CAG CTC CAA TAT and L21), for SOC_{1KC} (forward primer L13: GCT CTA GAG CGC AGC AAA CAT GAT G and L21), for SSO31 (L11 and reverse primer L24: CGG GAT CCA TGG TAT CTT GCA TAC), for SSO14 (L11 and reverse primer L25: CGG GAT CCA CTT TAT CTT TTG CTT G), and for SSO4, SSO11, SSO36 (L11 and L21). For the AGL24:RFP fusion construct, the *AGL24* cDNA fragment was amplified by RT-PCR with forward primer 5′-GCT CTA GAA TGG CGA GAG AG-3′ and reverse primer 5′-CCG GAT CGT TTC CCA AGA TGG AAG CCC-3′, and the product

was inserted into the *Xba*I and *Sma*I sites in the p326-RFP vector (Lee *et al.*, 2001).

Western blot analysis

For isolation of nuclear protein from different organs, each organ was collected from 100 young seedlings. The following nuclear isolation was based on a previously described method (Sheen, 1993). Harvested tissues were ground with liquid nitrogen, resuspended with 0.5 ml of nuclear enrichment buffer A [20 mM 2-amino-2-(hydroxymethyl)-1,3-propandiol (TRIS)-Cl, pH 7.0, 25% glycerol, 2.5 mM $MgCl_2$, 30 mM β-mercaptoethanol, 1× Complete protease inhibitor (Roche, http://www.roche.com/), 0.05% Triton X-100] and filtered through two layers of Miracloth (Calbiochem, http://emdbiosciences.com/). The filtrates were centrifuged at 2000 ***g*** at 4°C for 10 min. The soluble fractions were taken for cytoplasmic fractions and the nuclear pellets were resuspended with 0.3 ml of nuclear enrichment buffer B [20 mM TRIS-Cl, pH 7.0, 25% glycerol, 2.5 mM $MgCl_2$, 30 mM β-mercaptoethanol, 1× Complete protease inhibitor (Roche), 1% Triton X-100], and centrifuged at 2000 ***g*** at 4°C for 10 min. After centrifugation, the pellets were resuspended with 50 μl of 2× protein sample buffer and incubated for 10 min at room temperature. Then, the samples were boiled for 5 min and loaded onto 12% SDS-PAGE gels. The proteins were detected using anti-MYC (9E10, Santa Cruz Biotechnology, http://www.scbt.com) and anti-HA (F-7, Santa Cruz) antibody. The anti-H3 antibody (Millipore, http://www.millipore.com) was used to check the efficiency of the nuclear isolation process.

Chromatin immunoprecipitation

A total of 0.8 g of 9-day-old seedlings were used for chromatin immunoprecipitation, following a previously described method (Lee *et al.*, 2007a,b). The ChIP products were resuspended with 50 μl of TE, and 1 μl was used for PCR. Sonicated input DNA (0.5%) was used for PCR as a quantitative control. The primers for the regions spanning the LFY promoter are as follows (a, 5′-CCG GAT CCA TCC ATT TTT CGC AAA GG-3′ and 5′-CCG GAT CCA TCT GTT CTA AAG CCT CC-3′; b, 5′-CCG GAT CCG CAA AGT GTA GTT CGG TC-3′ and 5′-CCG GAT CCT TGA CGT CTC ACT CCC TC-3′; c, 5′-CCG GAT CCG TTG TAA ACT TGT AAT GT-3′ and 5′-CCG GAT CCT AAA GTG GGG AAA AAA GC-3′; d, 5′-CCG GAT CCC CCA TAT GTC CAA TCC CA-3′ and 5′-CCG GAT CCA TCT ATC TGC GTT TTA GG-3′; e, 5′-CCG GAT CCG ACC TCC TCT CCT TCT GG-3′ and 5′-CCG GAT CCA AAC TTT AAC TGT ATT GG-3′; f, 5′-CCG GAT CCC GGG CTT CTG CAA AGA TT-3′and 5′-CCG GAT CCA ACC ATT CCA CCA TTT GG-3′; g, 5′-CCG GAT CCC AAT CTA TCG TAA CAA AT-3′, 5′-CCG GAT CCC ATA ATT TGA CAC GTA GG-3′; h, 5′-CCG GAT CCC ACC ACA GTG AAA ACC CT-3′ and 5′-CCG GAT CCA TAA TCT ATT TTT CTC TC-3′). A 1/200 concentration of anti-SOC1 serum in the ChIP binding buffer was used for the immunoprecipitation. Anti-SOC1 sera were raised in rabbits by repeated injection of 100 μg of GST fusion of $SOC1_{IKC}$. Recombinant proteins were produced in BL21 cells and purified using the manufacturer's protocols (Amersham, http://www5.amershambiosciences.com/).

Protoplast transient expression assay

The well-expanded rosette leaves of L*er* plants grown for 4 weeks in long-day conditions were collected for the isolation. The transformation of protoplasts was performed as described (Yoo *et al.*, 2007). Protoplasts were co-transformed with both GFP and RFP fusion constructs, each with about 10 μg of plasmid DNA (prepared using the Qiagen Plasmid Midi Kit, http://wwwqiagen.com/) and incubated at 22°C. After 12–16 h of transformation, protoplasts were observed with a confocal laser scanning microscope equipped with an argon/krypton laser (Bio-Rad, http://www.bio-rad.com/). The GFP and RFP fusion proteins were excited at 488 and 568 nm, and the green and red fluorescence signals were filtered with HQ515/30 and HQ600/50 emission filters, respectively. The auto-fluorescence of chlorophylls was excited at 568 nm and emitted with the E600LP filter. The merged signals were obtained using a Confocal Assistant 4.02 (Todd Clark Brelje, freeware).

Analysis of gene expression

Total RNA was extracted from each organ of the Arabidopsis seedlings and adult plants using TRIzol reagent (Sigma-Aldrich, http://www.sigmaaldrich.com/). One microgram of total RNA from each tissue was reverse-transcribed with oligo-$dT_{12–18}$ (Fermentas, http://www.fermentas.com/) in a 20-μl reaction mixture using MMLV Reverse Transcriptase (Fermentas). After reverse transcription, PCR was performed using 1 μl of the first-strand cDNA sample with 25 pmol of the primers in a 25 μl reaction. The PCR conditions were as follows: 94°C (3 min), 22–35 cycles of 94°C (30 sec), 57°C (30 sec), 72°C (30 sec) and 72°C (10 min). The PCR products were electrophoresed on 1.5% of agarose gels, blotted to a NYTRAN-PLUS membrane (Whatman, http://www.whatman.com), and hybridized with ^{32}P-labelled probes. The RT-PCR was repeated at least three times with independently harvested samples. The primers for β-*tubulin* (*TUB2*) and *SOC1* have been described previously (Lee *et al.*, 2000). For *AGL24*, two primers, 5′-GTC TTC ATG CAA GTA ACA TCA ACA AA-3′ and 5′-TCC ATC GAA GTC AAC TCT GCT GGA TC-3′; for *AP1*, two primers, 5′-TTG AAC GCT ATG AGA GGT AC-3′ and 5′-TTT TCC CTC TCC TTG ATC TG-3′; for *LFY*, two primers, 5′-CTT TCG TTG GGA GCT TCT TG-3′ and 5′-CTG CGT CCC AGT AAC CAC TT-3′ were used.

Acknowledgements

We thank Dr H. Yu for kindly providing the *35S-AGL24:6HA* seeds and for sharing unpublished information. This work was partially supported by the Korea Ministry of Science and Technology under the National Research Laboratory Program (2006-01952), a grant from Global Research Laboratory Program (2006-03870), a grant from Seoul R&BD Program and a grant from the Korea Science and Engineering Foundation through the Plant Metabolism Research Center, Kyung Hee University. JL, MO and HP were supported by the Brain Korea 21 program.

Supporting Information

Additional supporting information may be found in the online version of this article.

Figure S1. The subcellular localization of SOC1:GFP in *35S-SOC1:GFP* transgenic plants.

Figure S2. The amino acid sequence alignment in MIKC type MADS box proteins.

Figure S3. Confocal laser scanning microscopy of Arabidopsis protoplasts expressing mutated forms of SOC1 protein in *sso* mutants and AGL24.

Please note: Blackwell Publishing are not responsible for the content or functionality of any supporting materials supplied by the authors. Any queries (other than missing material) should be directed to the corresponding author for the article.

References

Alvarez-Buylla, E.R., Liljegren, S.J., Pelaz, S., Gold, S.E., Burgeff, C., Ditta, G.S., Vergara-Silva, F. and Yanofsky, M.F. (2000) MADS-box gene evolution beyond flowers: expression in pollen, endosperm, guard cells, roots and trichomes. *Plant J.* **24**, 457–466.

Amasino, R.M. (2005) Vernalization and flowering time. *Curr. Opin. Biotechnol.* **16**, 154–158.

Arabidopsis Genome Initiative (2000) Analysis of the genome sequence of the flowering plant *Arabidopsis thaliana*. *Nature*, **408**, 796–815.

Blazquez, M.A. and Weigel, D. (2000) Integration of floral inductive signals in Arabidopsis. *Nature*, **404**, 889–892.

Cho, S., Jang, S., Chae, S., Chung, K.M., Moon, Y.H., An, G. and Jang, S.K. (1999) Analysis of the C-terminal region of Arabidopsis thaliana APETALA1 as a transcription activation domain. *Plant Mol. Biol.* **40**, 419–429.

Conti, L. and Bradley, D. (2007) TERMINAL FLOWER1 is a mobile signal controlling Arabidopsis architecture. *Plant Cell*, **19**, 767–778.

Egea-Cortines, M., Saedler, H. and Sommer, H. (1999) Ternary complex formation between the MADS-box proteins SQUAMOSA, DEFICIENS and GLOBOSA is involved in the control of floral architecture in *Antirrhinum majus*. *EMBO J.* **18**, 5370–5379.

Fan, H.Y., Hu, Y., Tudor, M. and Ma, H. (1997) Specific interactions between the K domains of AG and AGLs, members of the MADS domain family of DNA binding proteins. *Plant J.* **12**, 999–1010.

Ferrario, S., Busscher, J., Franken, J., Gerats, T., Vandenbussche, M., Angenent, G.C. and Immink, R.G. (2004) Ectopic expression of the petunia MADS box gene *UNSHAVEN* accelerates flowering and confers leaf-like characteristics to floral organs in a dominant-negative manner. *Plant Cell*, **16**, 1490–1505.

de Folter, S. and Angenent, G.C. (2006) *trans* meets *cis* in MADS science. *Trends Plant Sci.* **11**, 224–231.

de Folter, S., Immink, R.G., Kieffer, M. *et al.* (2005) Comprehensive interaction map of the Arabidopsis MADS box transcription factors. *Plant Cell*, **17**, 1424–1433.

Gregis, V., Sessa, A., Colombo, L. and Kater, M.M. (2006) AGL24, SHORT VEGETATIVE PHASE, and APETALA1 redundantly control *AGAMOUS* during early stages of flower development in Arabidopsis. *Plant Cell*, **18**, 1373–1382.

Han, A., Pan, F., Stroud, J.C., Youn, H.D., Liu, J.O. and Chen, L. (2003) Sequence-specific recruitment of transcriptional co-repressor Cabin1 by myocyte enhancer factor-2. *Nature*, **422**, 730–734.

Hayama, R. and Coupland, G. (2003) Shedding light on the circadian clock and the photoperiodic control of flowering. *Curr. Opin. Plant Biol.* **6**, 13–19.

Hepworth, S.R., Valverde, F., Ravenscroft, D., Mouradov, A. and Coupland, G. (2002) Antagonistic regulation of flowering-time gene *SOC1* by CONSTANS and FLC via separate promoter motifs. *EMBO J.* **21**, 4327–4337.

Honma, T. and Goto, K. (2001) Complexes of MADS-box proteins are sufficient to convert leaves into floral organs. *Nature*, **409**, 525–529.

Huang, H., Mizukami, Y., Hu, Y. and Ma, H. (1993) Isolation and characterization of the binding sequences for the product of the Arabidopsis floral homeotic gene *AGAMOUS*. *Nucleic Acids Res.* **21**, 4769–4776.

Immink, R.G. and Angenent, G.C. (2002) Transcription factors do it together: the hows and whys of studying protein-protein interactions. *Trends Plant Sci.* **7**, 531–534.

Jeon, J.-S., Jang, S., Lee, S. *et al.* (2000) *leafy hull sterile1* is a homeotic mutation in a rice MADS box gene affecting rice flower development. *Plant Cell*, **12**, 871–884.

Krizek, B.A. and Meyerowitz, E.M. (1996) Mapping the protein regions responsible for the functional specificities of the Arabidopsis MADS domain organ-identity proteins. *Proc. Natl Acad. Sci. USA*, **93**, 4063–4070.

Lee, H., Suh, S.S., Park, E., Cho, E., Ahn, J.H., Kim, S.G., Lee, J.S., Kwon, Y.M. and Lee, I. (2000) The AGAMOUS-LIKE 20 MADS domain protein integrates floral inductive pathways in Arabidopsis. *Genes Dev.* **14**, 2366–2376.

Lee, Y.J., Kim, D.H., Kim, Y.-W. and Hwang, I. (2001) Identification of a signal that distinguishes between the chloroplast outer envelope membrane and the endomembrane system in vivo. *Plant Cell*, **13**, 2175–2190.

Lee, J., He, K., Stolc, V., Lee, H., Figueroa, P., Gao, Y., Tongprasit, W., Zhao, H., Lee, I. and Deng, X.W. (2007a) Analysis of transcription factor HY5 genomic binding sites revealed its hierarchical role in light regulation of development. *Plant Cell*, **19**, 731–749.

Lee, J.H., Yoo, S.J., Park, S.H., Hwang, I., Lee, J.S. and Ahn, J.H. (2007b) Role of SVP in the control of flowering time by ambient temperature in Arabidopsis. *Genes Dev.* **21**, 397–402.

Liu, C., Zhou, J., Bracha-Drori, K., Yalovsky, S., Ito, T. and Yu, H. (2007) Specification of Arabidopsis floral meristem identity by repression of flowering time genes. *Development*, **134**, 1901–1910.

McGonigle, B., Bouhidel, K. and Irish, V.F. (1996) Nuclear localization of the Arabidopsis APETALA3 and PISTILLATA homeotic gene products depends on their simultaneous expression. *Genes Dev.* **10**, 1812–1821.

Michaels, S.D., Ditta, G., Gustafson-Brown, C., Pelaz, S., Yanofsky, M. and Amasino, R.M. (2003) *AGL24* acts as a promoter of flowering in Arabidopsis and is positively regulated by vernalization. *Plant J.* **33**, 867–874.

Moon, J., Suh, S.S., Lee, H., Choi, K.R., Hong, C.B., Paek, N.C., Kim, S.G. and Lee, I. (2003) The *SOC1* MADS-box gene integrates vernalization and gibberellin signals for flowering in Arabidopsis. *Plant J.* **35**, 613–623.

Moon, J., Lee, H., Kim, M. and Lee, I. (2005) Analysis of flowering pathway integrators in Arabidopsis. *Plant Cell Physiol.* **46**, 292–299.

Onouchi, H., Igeno, M.I., Perilleux, C., Graves, K. and Coupland, G. (2000) Mutagenesis of plants overexpressing *CONSTANS* demonstrates novel interactions among Arabidopsis flowering-time genes. *Plant Cell*, **12**, 885–900.

Parcy, F. (2005) Flowering: a time for integration. *Int. J. Dev. Biol.* **49**, 585–593.

Pellegrini, L., Tan, S. and Richmond, T.J. (1995) Structure of serum response factor core bound to DNA. *Nature*, **376**, 490–498.

Riechmann, J.L. and Meyerowitz, E.M. (1997a) Determination of floral organ identity by Arabidopsis MADS domain homeotic proteins AP1, AP3, PI, and AG is independent of their DNA-binding specificity. *Mol. Biol. Cell*, **8**, 1243–1259.

Riechmann, J.L. and Meyerowitz, E.M. (1997b) MADS domain proteins in plant development. *Biol. Chem.* **378**, 1079–1101.

Riechmann, J.L. and Ratcliffe, O.J. (2000) A genomic perspective on plant transcription factors. *Curr. Opin. Plant Biol.* **3**, 423–434.

Riechmann, J.L., Krizek, B.A. and Meyerowitz, E.M. (1996a) Dimerization specificity of Arabidopsis MADS domain homeotic proteins APETALA1, APETALA3, PISTILLATA, and AGAMOUS. *Proc. Natl Acad. Sci. USA*, **93**, 4793–4798.

Riechmann, J.L., Wang, M. and Meyerowitz, E.M. (1996b) DNA-binding properties of Arabidopsis MADS domain homeotic proteins APETALA1, APETALA3, PISTILLATA and AGAMOUS. *Nucleic Acids Res.* **24**, 3134–3141.

Rubio, V., Shen, Y., Saijo, Y., Liu, Y., Gusmaroli, G., Dinesh-Kumar, S.P. and Deng, X.W. (2005) An alternative tandem affinity purifi-

cation strategy applied to Arabidopsis protein complex isolation. *Plant J.* **41**, 767–778.

Samach, A., Onouchi, H., Gold, S.E., Ditta, G.S., Schwarz-Sommer, Z., Yanofsky, M.F. and Coupland, G. (2000) Distinct roles of CONSTANS target genes in reproductive development of Arabidopsis. *Science*, **288**, 1613–1616.

Santelli, E. and Richmond, T.J. (2000) Crystal structure of MEF2A core bound to DNA at 1.5 A resolution. *J. Mol. Biol.* **297**, 437–449.

Searle, I., He, Y., Turck, F., Vincent, C., Fornara, F., Krober, S., Amasino, R.A. and Coupland, G. (2006) The transcription factor FLC confers a flowering response to vernalization by repressing meristem competence and systemic signaling in Arabidopsis. *Genes Dev.* **20**, 898–912.

Sheen, J. (1993) Protein phosphatase activity is required for light-inducible gene expression in maize. *EMBO J.* **12**, 3497–3505.

Shiraishi, H., Okada, K. and Shimura, Y. (1993) Nucleotide sequences recognized by the AGAMOUS MADS domain of Arabidopsis thaliana in vitro. *Plant J.* **4**, 385–398.

Simpson, G.G. and Dean, C. (2002) Arabidopsis, the Rosetta stone of flowering time? *Science*, **296**, 285–289.

Sung, Z.R., Chen, L., Moon, Y.H. and Lertpiriyapong, K. (2003) Mechanisms of floral repression in Arabidopsis. *Curr. Opin. Plant Biol.* **6**, 29–35.

Tan, S. and Richmond, T.J. (1998) Crystal structure of the yeast MATalpha2/MCM1/DNA ternary complex. *Nature*, **391**, 660–666.

Theissen, G., Becker, A., Di Rosa, A., Kanno, A., Kim, J.T., Munster, T., Winter, K.U. and Saedler, H. (2000) A short history of MADS-box genes in plants. *Plant Mol. Biol.* **42**, 115–149.

Yang, Y., Fanning, L. and Jack, T. (2003) The K domain mediates heterodimerization of the Arabidopsis floral organ identity proteins, APETALA3 and PISTILLATA. *Plant J.* **33**, 47–59.

Yoo, S.D., Cho, Y.H. and Sheen, J. (2007) Arabidopsis mesophyll protoplasts: a versatile cell system for transient gene expression analysis. *Nat. Protoc.* **2**, 1565–1572.

Yu, H., Xu, Y., Tan, E.L. and Kumar, P.P. (2002) AGAMOUS-LIKE 24, a dosage-dependent mediator of the flowering signals. *Proc. Natl Acad. Sci. USA*, **99**, 16336–16341.

Yu, H., Ito, T., Wellmer, F. and Meyerowitz, E.M. (2004) Repression of AGAMOUS-LIKE 24 is a crucial step in promoting flower development. *Nat. Genet.* **36**, 157–161.

